[10] L. P. Schimidt and T. Itoh, "Spectral domain analysis of dominant and higher order modes in fin-lines," *IEEE Trans. Microwave Theory Tech.*, vol. MTT-28, pp. 981–985, Sept. 1980.
[11] H. Hofmann, "Calculation of quasi-planer lines for mm-wave application," in *Proc. 1977 Int. Microwave Conf.*, pp. 381–384.
[12] R. P. Hecklen, "A near-optimum matching section without discontinuities," *IEEE Trans. Microwave Theory Tech.*, vol. MTT-20, pp. 734–739, Nov. 1972.
[13] J. H. Hinken, "Simplified analysis and synthesis of fin-line tapers," *Arch. Elek. Übertragung.*, vol. 37 pp. 375–380, Nov/Dec. 1983.
[14] P. Wahi and K. C. Gupta, "Effect of diode parameters on reflection-type phase shifters," *IEEE Trans. Microwave Theory Tech.*, vol. MTT-24, pp. 619–621, Sept. 1976.
[15] R. C. Compton and D. B. Ruthledge, *Puff: Microwave Computer Aided Design*. (Manual and Software available from authors.)

A 13 GHz YIG Film Tuned Oscillator for VSAT Applications

'YASUYUKI MIZUNUMA, YOSHIKAZU MURAKAMI, HIROYUKI NAKANO, TAKAHIRO OHGIHARA, AND TSUTOMU OKAMOTO

***Abstract*—A 13 GHz tunable oscillator using YIG film grown by LPE has been developed. A very low phase noise of −93 dBc/Hz at 10 kHz from the carrier and an output power of 11 dBm have been achieved over the entire tuning range of 500 MHz. With excellent linear tuning characteristics, this oscillator is ideal for use as a frequency-agile synthesized local oscillator in a very small aperture terminal system.**

I. Introduction

Today's *Ku*-band very small aperture terminal (VSAT) will make it possible for many more people to use commercial satellite communication services. We have utilized YIG film grown by LPE to develop a compact, low-cost, high-performance *Ku*-band tunable oscillator for use in a VSAT system [1]–[3].

As is widely recognized, local oscillator phase noise is a critical parameter in the bit error rate (*BER*) performance of a digital earth terminal [4]. From the high unloaded Q of the uniform precession mode of a YIG resonator, a very low phase noise of −93 dBc/Hz at 10 kHz from the carrier has been achieved over the entire tuning range of 500 MHz.

A compact magnetic circuit has been constructed of a permanent magnet supplying the dc magnetic field required to resonate the YIG film at 13 GHz, and a small tuning coil covering the 500 MHz tuning range. By appropriate design of the gallium substitution in the YIG film, temperature compensation between the permanent magnet and the YIG film has been achieved [1]. This approach enabled us to realize a YIG-tuned oscillator (YTO) of compact size, low power consumption for biasing field, and rapid tuning response.

Because of its low phase noise, high output power, and linear tuning characteristics, this oscillator is ideal for use as a frequency-agile synthesized local oscillator in a VSAT system. As the local oscillator selects the different channels in the up-conversion and down-conversion RF sections, it makes the construction of the earth terminal much simpler than that of a terminal using a fixed-frequency dielectric resonator local oscillator (DRO) and block conversion.

This paper will first describe the fabrication of the tunable oscillator using YIG film. The design criteria of the YIG film resonator and the output matching network to achieve low phase noise and high output power will then be discussed. The relation between phase noise, temperature, and biasing voltage V_{ds} will then be described. Finally, the tuning characteristic and the drift of the frequency and output power over the temperature range from −30°C to +60°C will be presented.

Manuscript received April 5, 1988; revised August 1, 1988.
The authors are with the Sony Corporation Research Center, 174 Fujitsukacho, Hodogaya-ku, Yokohama, 240 Japan.
IEEE Log Number 8823770.

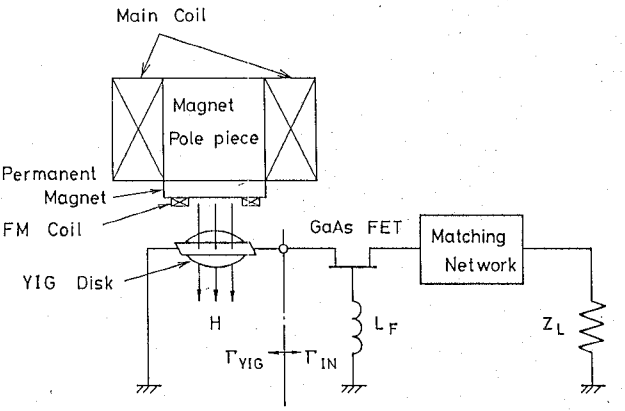

Fig. 1. Schematic structure of the complete YTO.

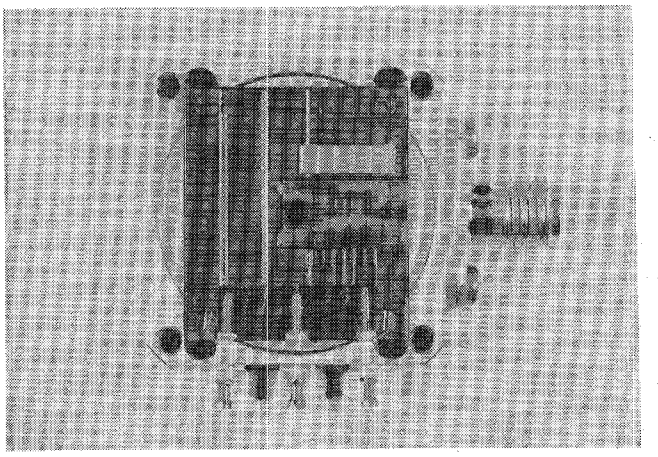

Fig. 2. Oscillator MIC.

II. Oscillator Fabrication

The schematic structure of the complete YIG film tuned oscillator and its circuit are illustrated in Figs. 1 and 2, respectively. The GaAs FET is in the common-gate configuration with the source connected to the YIG film resonator and the drain connected to the output matching circuit [5].

Fig. 3 shows the trajectory of the inverse of the input small-signal reflection coefficient Γ_{in} with frequency, and a typical reflection coefficient loop Γ_{YIG} resonating at 13 GHz. The condition for the onset of oscillation is that Γ_{in}^{-1} be encircled by Γ_{YIG}, and stable oscillation is realized when the condition $\Gamma_{in}^{-1}(A) = \Gamma_{YIG}$ is satisfied with the increase of signal level A of the GaAs FET.

0018-9480/88/1200-1885$01.00 ©1988 IEEE

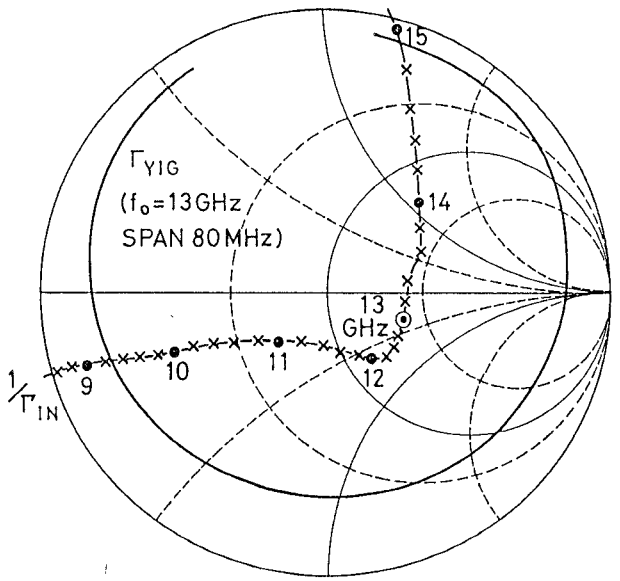

Fig 3 Reflection coefficient Γ_{YIG} and the trajectory of Γ_{in}^{-1}.

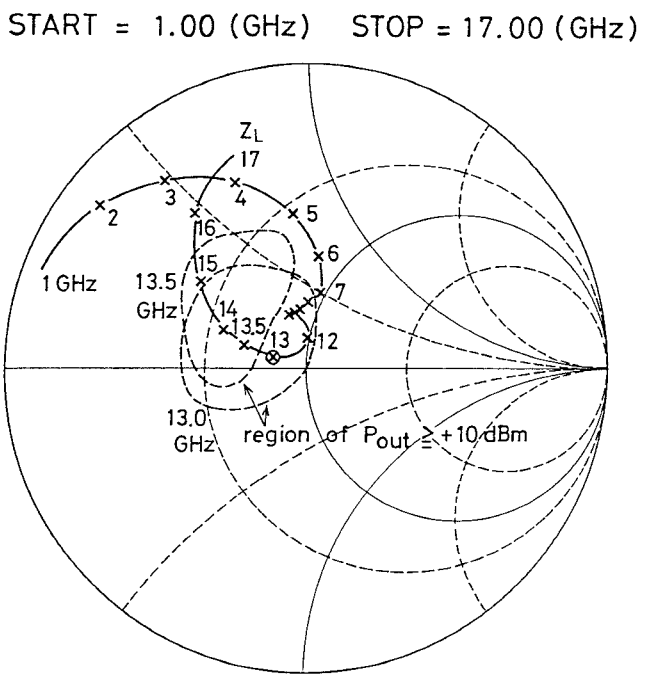

Fig. 4. Rieke diagram (constant output power) and the locus of the load circuit.

A suspended substrate stripline was adopted in order to avoid the spurious oscillation caused by the feedback from the source line.

The YIG disk resonator was normally magnetized by the magnetic circuit. The dc magnetic field of about 5600 Oe required to resonate the YIG disk at 13 GHz was supplied by the permanent magnet, and the tuning magnetic field of about 180 Oe required to cover 500 MHz was supplied by the coil current.

III. YIG Resonator Design

In order to realize a low-phase-noise, high-output oscillator, a resonator which has high Q, a large loop diameter, and high critical power is required. As a resonator to stabilize the oscillation frequency, a YIG resonator which has a specific critical power was used. Once the input power to the YIG resonator exceeds the critical power, the resonance is subjected to the nonlinear effect of the YIG, and the phase noise of the oscillator increases rapidly [6]. If the critical power were not sufficiently high, we would have to find a compromise between low phase noise and high output power by adjusting the bias and the Q, the loop diameter, and the critical power of the resonator [7].

The new resonator has a very high critical power, 22 dBm, while high power instability has been eliminated. The unloaded Q, the loaded Q, and the loop diameter of the resonator were 2470, 380, and 1.70, respectively.

IV. Load Circuit Design

The performance of the new YIG resonator suggests the possibility of realizing a low-phase-noise, high-output oscillator if there is an optimum load circuit. We designed the load circuit utilizing the measured Rieke diagram shown in Fig. 4.

V. Noise Characteristics

We concentrated our efforts on realizing a high-output YTO with a phase noise below -90 dBc/Hz at 10 kHz from the carrier under the following conditions: tuning range from 13 GHz to 13.5 GHz; temperature range -30°C to $+60$°C; V_{ds} variation ± 10 percent.

We first measured the variation in the phase noise at room temperature caused by a ± 10 percent variation in V_{ds} and with two different types of YTO's, a free-running YTO (FRYTO) and

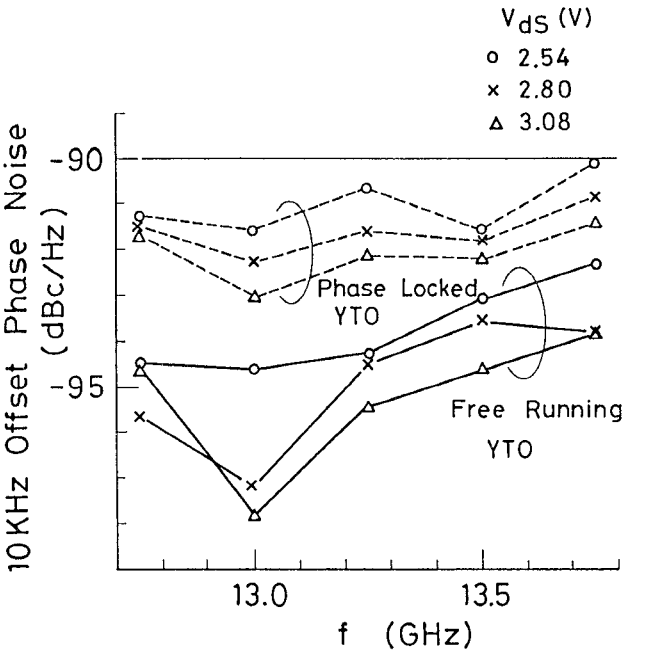

Fig 5. 10 kHz offset phase noise of FRYTO and PLYTO at room temperature

a phase-locked YTO (PLYTO). As can be seen in Fig. 5, the larger the V_{ds} applied to the FET, the lower the phase noise becomes. The minimum phase noise at 10 kHz from the carrier was -98 dBc/Hz. This value was obtained when the FRYTO was measured by the delay-line discriminator method and a carrier noise test set was employed under the conditions of $f = 13$ GHz, $V_{ds} = 3.08$ V, and $V_{gs} = 0$ V. The phase noise of the FRYTO 10 kHz offset from the carrier was below -93 dBc/Hz over the entire tuning range from 13 GHz to 13.5 GHz, even if we consider the ± 10 percent variation of V_{ds}. Fig. 6 shows the measured phase noise characteristics when the oscillator was

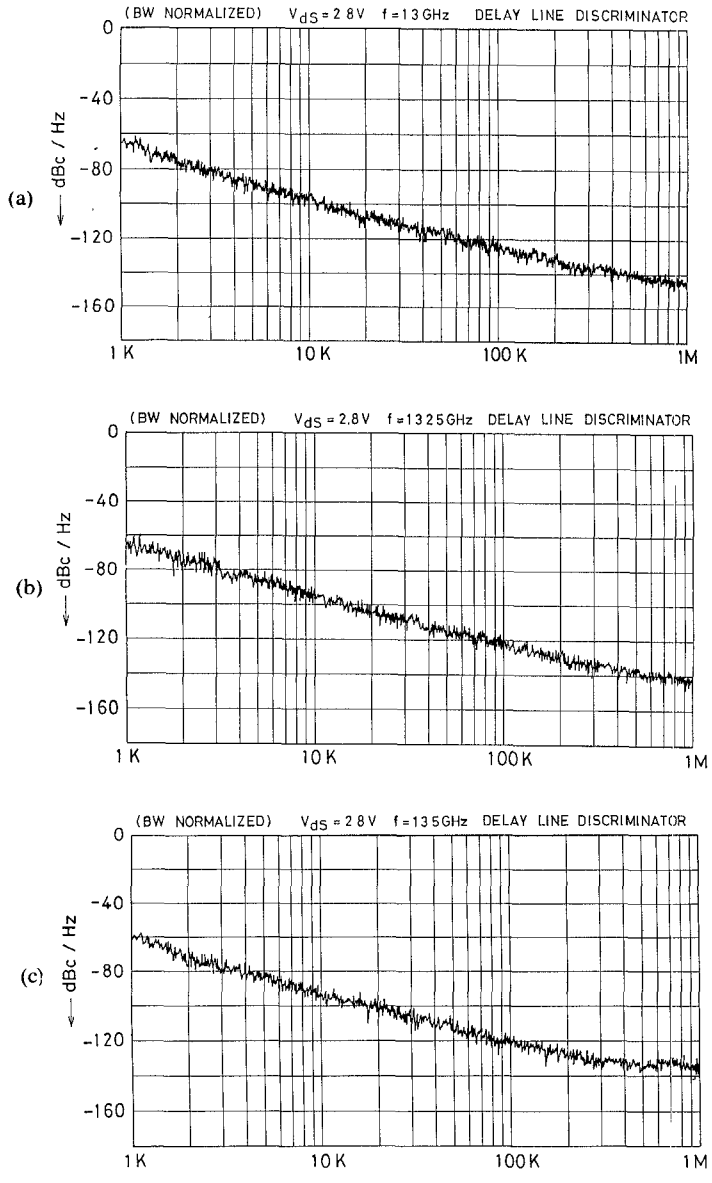

Fig 6. SSB phase noise of FRYTO for 13–13.5 GHz band. (a) $f = 13$ GHz. (b) $f = 13.25$ GHz (c) $f = 13.5$ GHz.

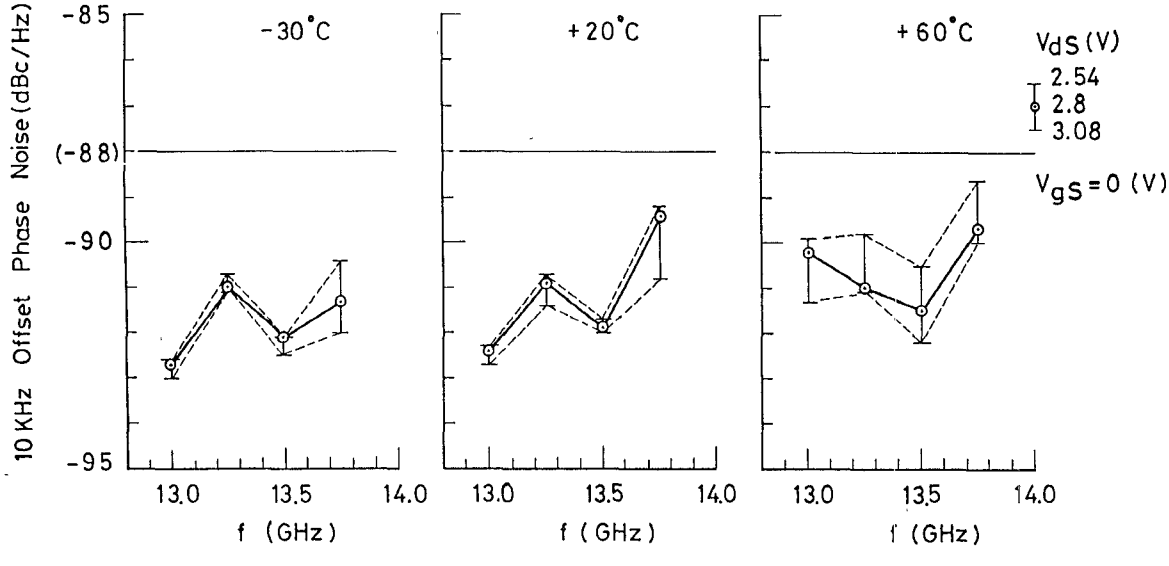

Fig. 7. 10 kHz offset phase noise of PLYTO at −30°C, +20°C, and +60°C.

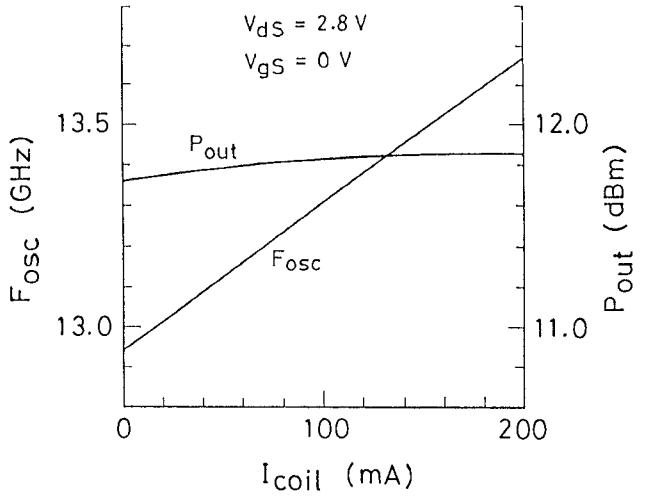

Fig. 8. Tuning characteristics of the YTO.

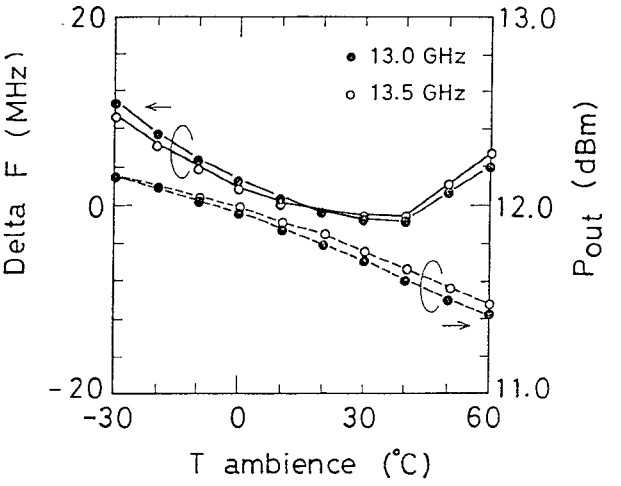

Fig 9 Temperature dependence of oscillation frequency and output power at 13–13 5 GHz band

turned to 13 GHz, 13.25 GHz, and 13.5 GHz under the bias conditions of $V_{ds} = 2.8$ V and $V_{gs} = 0$ V.

Though the phase noise data of the PLYTO were acquired using a spectrum analyzer, those of the FRYTO was acquired using the delay-line discriminator method and employing a carrier noise test set. We incorporated the YTO into the PLL to simplify the phase noise measurement. The loop parameters of the PLL were chosen so as not to allow the phase noise to increase significantly compared with the FRYTO [8]. From Fig. 5, we can estimate that the 10 kHz offset phase noise of the PLYTO is at least 2 dB worse than that of the FRYTO. Fig. 7 shows the phase noise of the PLYTO at −30°C, +20°C, and +60°C. As noted above, we can deduct 2 dB from this phase noise data for the FRYTO. Though the phase noise at +60°C was higher than at other temperatures, the maximum phase noise at 10 kHz from the carrier was below −88 dBc/Hz, which corresponds to the phase noise below −90 dBc/Hz for the FRYTO.

VI. Other Characteristics

The tuning characteristics of the oscillator are shown in Fig. 8. The output power of the oscillator was over 11 dBm, the variation of the output power was about 0.1 dB, and the hysteresis of the oscillation frequency was less than 1 MHz over the tuning range from 13 GHz to 13.5 GHz.

Fig. 9 shows the variation of the oscillation frequency and of the output power with temperature. A small oscillation frequency drift of 12 MHz and a small oscillation output variation of 0.8 dB have been achieved over the temperature range from −30°C to +60°C.

The characteristics of the oscillator are summarized in Table I. The outside dimensions of the oscillator are shown in Fig. 10.

TABLE I

Frequency range	13.0–13.5 GHz
Output power	11 dBm
Output power variation	0.1 dB
SSB phase noise at 10 kHz offset	−93 dBc/Hz
Frequency drift over temperature (−30°C to +60°C)	12 MHz
Main Tuning Port Characteristics:	
Sensitivity	3.5 MHz/mA
3 dB bandwidth	45 kHz
Hysterisis	1 MHz
Input impedance (1 kHz)	6 Ω with series 20 mH

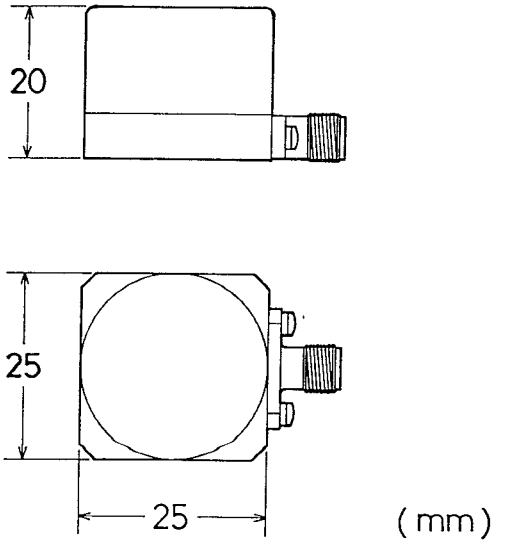

Fig. 10. Outside dimensions of the YTO.

VII. Conclusion

A 13 GHz tunable oscillator using YIG film grown by LPE has been developed. A very low phase noise of below −93 dBc/Hz at 10 kHz from the carrier has been achieved over the entire tuning range from 13 GHz to 13.5 GHz at room temperature. By using the PLL technique, a phase noise below −90 dBc/Hz at 10 kHz from the carrier has been confirmed from −30°C to +60°C and a V_{ds} variation of ±10 percent over the entire tuning range from 13 GHz to 13.5 GHz. The output power of the oscillator was over 11 dBm without an output buffer amplifier. This compact, low-cost, linear tuning characteristic is ideal for use as a frequency-agile synthesized local oscillator in a VSAT system.

Acknowledgment

The authors gratefully acknowledge the assistance of K. Nikura in this work. They wish to thank M. Saito and C. Isobe for providing the Ta_2O_5 MIS capacitors they developed. The authors

also wish to thank to T. Watanabe for his valuable suggestions on PLL circuits. Finally, they would like to thank Dr. T. Yamada for his helpful suggestions and encouragement.

REFERENCES

[1] Y. Murakami and S. Itoh, "A bandpass filter using YIG film grown by LPE," in *IEEE-MTT-S Int. Microwave Symp. Dig.*, 1985, pp. 285–288.
[2] Y. Murakami, T. Ohgihara, and T. Okamoto, "A 0.5–4.0 GHz tunable bandpass filter using YIG film grown by LPE," in *IEEE-MTT-S Int. Microwave Symp. Dig.*, 1987, pp. 371–372.
[3] T. Ohgihara, Y. Murakami, and T. Okamoto, "A 0.5–2.0 GHz tunable bandpass filter using YIG film grown by LPE," *IEEE Trans. Magn.*, vol. MAG-23, no. 5, pp. 3745–3747, 1987.
[4] N. K. Osbrink, "Earth-terminal design benefits from MMIC technology," *Microwave Syst. News*, vol. 16, Aug. 1986.
[5] J. C. Papp and Y. Y. Koyano, "An 8–18-GHz YIG-tuned FET oscillator," *IEEE Trans. Microwave Theory Tech.*, vol. MTT-28, pp. 762–767, July 1980.
[6] B. Lax and K. J. Button, *Microwave Ferrites and Ferrimagnetics*. New York: McGraw Hill, 1962.
[7] Y. Mizunuma, T. Ohgihara, H. Nakano, T. Okamoto, and Y. Murakami, "A 13-GHz YIG-film tuned oscillator for VSAT applications," in *IEEE MTT-S Int. Microwave Symp. Dig.*, 1988, pp. 1085–1088.
[8] F. M. Gardner, *Phaselock Techniques*. New York: Wiley, 1979.

Full-Wave Analysis of Coupled Finline Discontinuities

GIOVANNI SCHIAVON, PIERO TOGNOLATTI, MEMBER, IEEE, AND ROBERTO SORRENTINO, SENIOR MEMBER, IEEE

***Abstract*—The general discontinuity problem of coupled finline sections is considered. Coupling may occur either along the sides of the slots (parallel coupled finlines) or through their ends (end-coupled finlines). A particular case is the inductive strip discontinuity already addressed in the literature. The analysis is carried out expanding the fields in terms of TE and TM modes in the transverse direction, according to the generalized transverse resonance method. End effects in coupled finline sections are pointed out. Computed results are in good agreement with both data from the literature and first experiments.**

I. INTRODUCTION

Finline discontinuities are still the objective of several investigations since not many data are available to the circuit designer. Accurate characterizations are of fundamental importance in establishing a reliable basis for the design of finline circuits.

An important class of discontinuity problems is that of coupled finline sections. They are used in a number of components, such as bandpass and bandstop filters and couplers. Both parallel coupling and end coupling may be realized. Such configurations are depicted in Fig. 1(a) and (b). Fig. 1(c) shows the geometry of the unilateral coupled finline structure. For analysis purposes, as discussed below, the structure is enclosed by two conducting planes perpendicular to the axial z direction.

In Fig. 1(a) two finline sections shorted at one end are coupled along the length s. In the discontinuity structure of Fig. 1(b) the two offset finline sections are shifted apart by a separation s so that the coupling occurs essentially through the line ends. The configuration of Fig. 1(b) can be considered as a special case of Fig. 1(a) by allowing the coupled length s to assume negative values. Negative s values thus correspond to a separation $|s|$ between the shorted ends of the finlines.

Manuscript received April 14, 1988; revised August 22, 1988
The authors are with the Dipartimento di Ingegneria Elettronica, Università Tor Vergata, Via Orazio Raimondo, I-00173 Roma, Italy.
IEEE Log Number 8824201.

Depending on the geometrical parameters, Fig. 1 can represent a number of different configurations. The uniform coupled line structure is recovered by letting $l_1 = l_2 = s > 0$. The inductive strip is a special case of Fig. 1(b) for zero line offset. Such a discontinuity problem has been studied by Koster and Jansen [1] and by Knorr and Deal [2] using the spectral-domain method.

The coupled finline discontinuity of Fig. 1 as well as the uniform coupled finline structure is analyzed in this paper using the generalized transverse resonance technique introduced in [3]. This method is well known, so it is only briefly reviewed in the next section. Results have been computed for both end-coupled and parallel coupled finlines and are presented in Section III. Good agreement has been found with the data available in [1] and [2] relative to the inductive strip.

II. METHOD OF ANALYSIS

The method is based on the computation of the resonant conditions of a finline cavity containing the discontinuity. The resonator is formed by placing electric (or magnetic) walls some distance apart from the discontinuity. Although higher order modes could be included in the analysis method, it is assumed that only the dominant mode can propagate in each finline section. Higher order modes excited at the discontinuity are assumed to have negligible amplitudes at the shorting planes. This condition can be met by shifting the terminal planes half a wavelength apart or by using magnetic walls a quarter of a wavelength apart. The discontinuity can then be modeled as a two-port network. Assuming losses to be negligible the two-port structure is characterized by three real parameters. For a given frequency, they are computed via the resonant lengths of the cavity, i.e., the distances l_1 and l_2. These are obtained by a field analysis of the finline cavity, as described below.

This method is equivalent to the tangent method [4] for measuring the equivalent circuit parameters of a discontinuity. It is observed that no characteristic impedance definition is needed since only normalized impedances enter the resonant condition. The computed impedances of the equivalent two-port are automatically normalized with respect to the characteristic impedances of the two finlines.

Simplification of the problem is obtained when the structure is symmetrical, thus $Z_{11} = Z_{22}$ (i.e., $w_1 = w_2$, $f_1 = f_2$ or $f_1 = b - f_2 - w_2$, Fig. 1). Two real quantities are sufficient to fully characterize the symmetrical discontinuity. Let the terminal planes be placed symmetrically ($l_1 = l_2$). Two types of resonance occur depending on whether the voltages at the ports are equal or opposite. The even (e) and odd (o) resonance conditions are

$$\begin{aligned} Z_e + Z_{11} - Z_{12} &= 0 \\ Z_o + Z_{11} + Z_{12} &= 0 \end{aligned} \tag{1}$$

where

$$Z_{e,o} = j \tan(\beta l_{e,o}) \tag{2}$$

are the normalized impedances seen from the discontinuity in the even or odd resonance condition, $\beta = \beta_1 = \beta_2$ is the phase constant of both finlines, and l_e and l_o are the even and odd resonant lengths, respectively. From (1) one obtains the impedance parameters of the discontinuity as

$$Z_{11} = -(Z_e + Z_o)/2 \qquad Z_{12} = -(Z_e - Z_o)/2. \tag{3}$$

0018-9480/88/1200-1889$01.00 ©1988 IEEE